Supplementary Data

Synergistically enhanced performance of transition-metal doped Ni_2P for supercapacitance and overall water splitting

Gwaza E. Ayom,[a] Malik D. Khan,[a,b] Jonghyun Choi[c], Ram K. Gupta,[c] Werner E. van Zyl,[d] Neerish Revaprasadu[a]*

[a]Department of Chemistry, University of Zululand, Private Bag X1001, KwaDlangezwa 3880, South Africa.

[b]Institute of Physical Chemistry, Polish Academy of Sciences, Kasprzaka 44/52, 01-224, Warsaw, Poland.

[c]Department of Chemistry, Pittsburg State University, Pittsburg, KS 66762, USA.

[d]School of Chemistry and Physics, University of KwaZuluNatal, Westville Campus, Durban, South Africa.

***Email:** RevaprasaduN@unizulu.ac.za

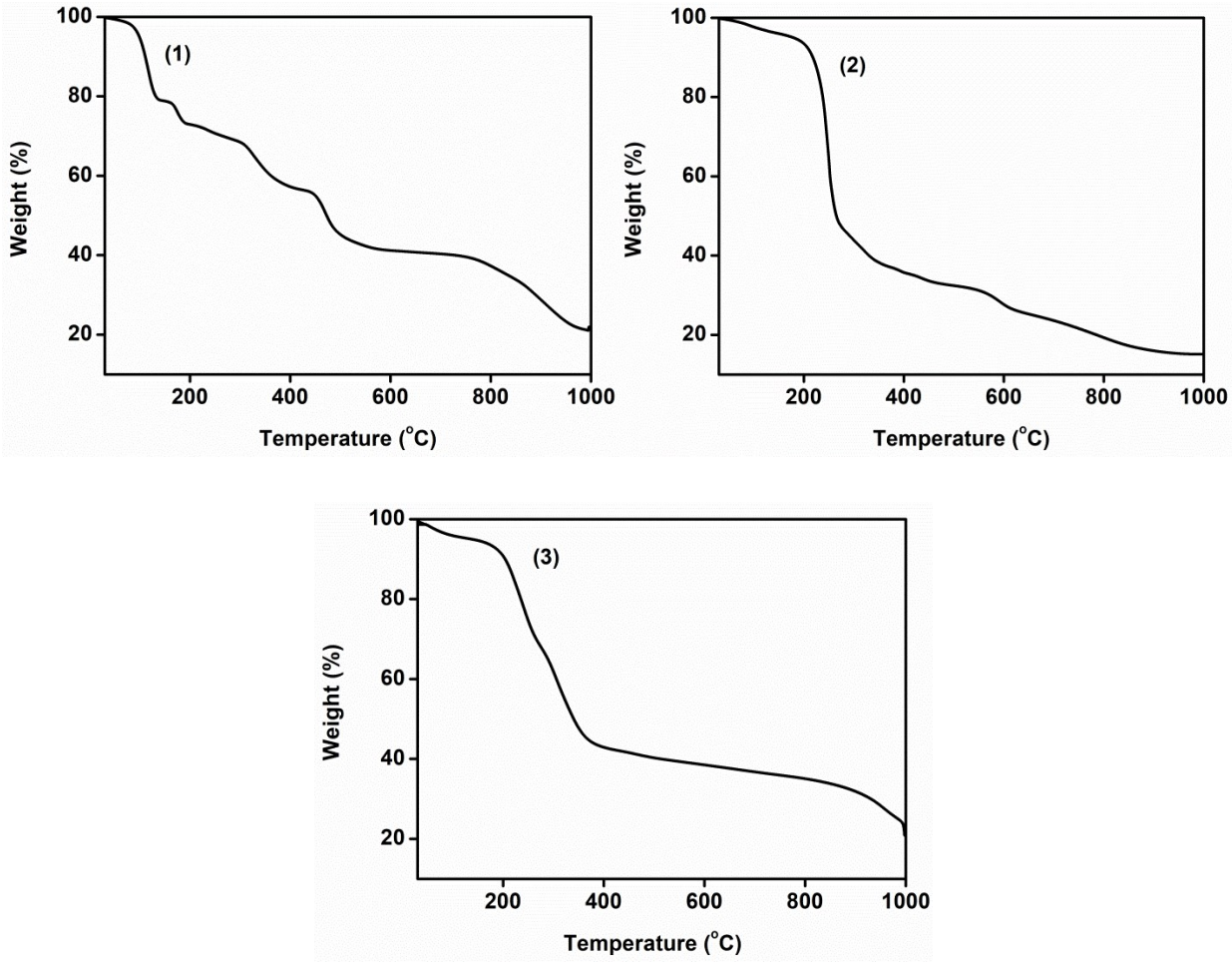

Figure S1: Thermographic curves for [Ni{$S_2P(OH)(4\text{-}CH_3OC_6H_4)\}_2$] (**1**), [Co{$S_2P(OC_4H_9)(4\text{-}CH_3OC_6H_4)\}_3$] (**2**) and [Fe{$S_2P(OH)(4\text{-}CH_3OC_6H_4)_3$] (**3**).

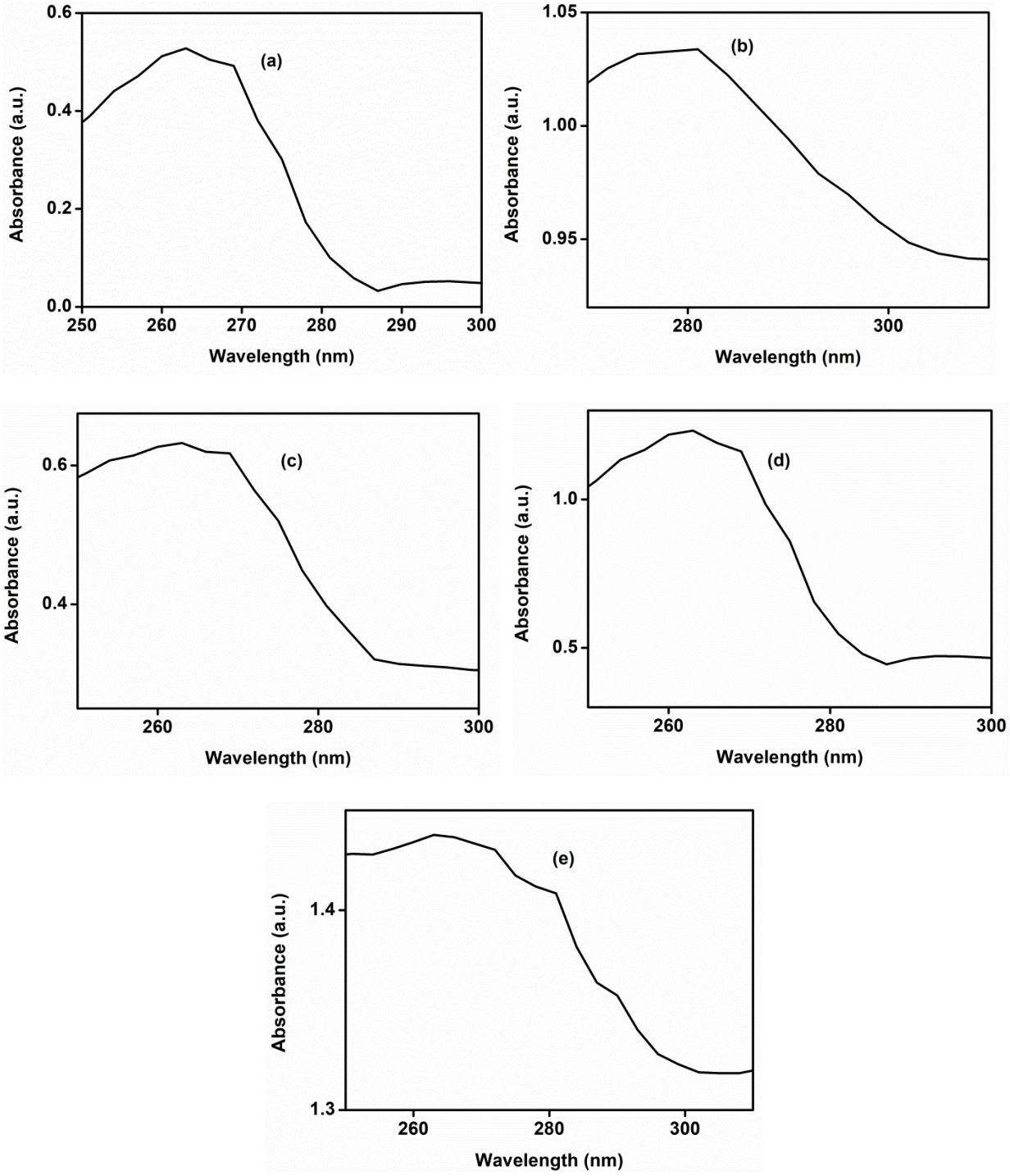

Figure S2: UV-vis absorption spectra of (a) Ni_2P (b) 5% Co-doped Ni_2P (c) 10% Co-doped Ni_2P (d) 5% Fe-doped Ni_2P and (e) 10% Fe-doped Ni_2P nanoparticles.

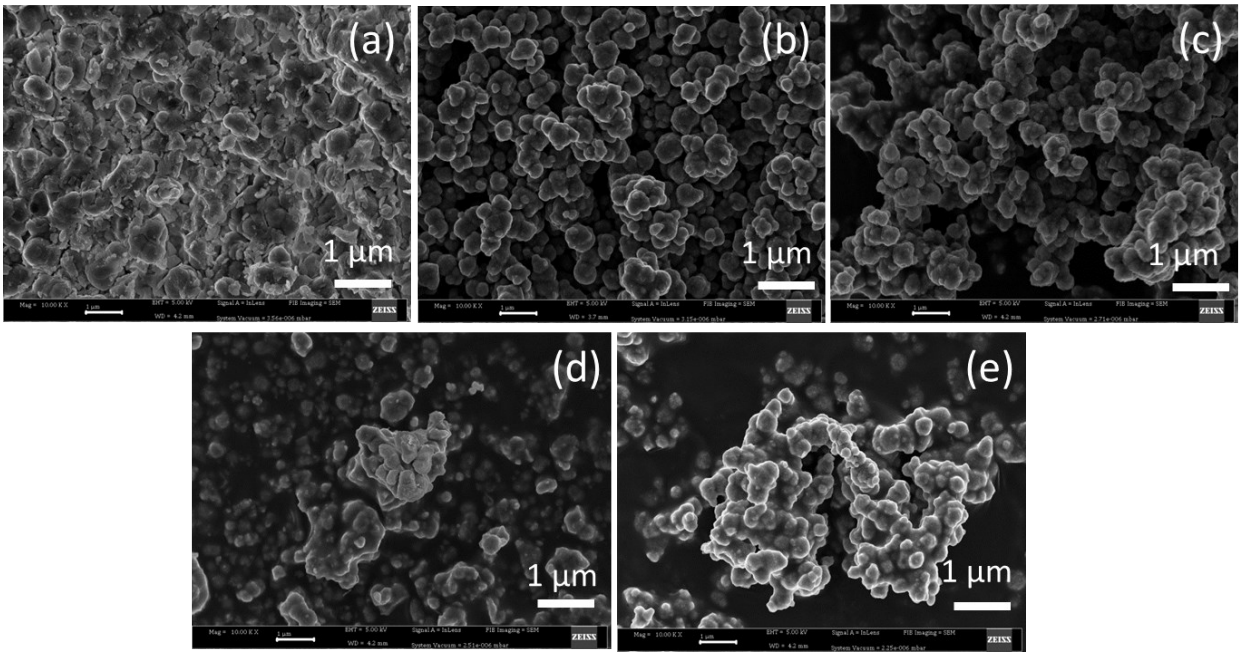

Figure S3: SEM images of (a) Ni_2P (b) 5% Co-doped Ni_2P, (c) 10% Co-doped Ni_2P, (d) 5% Fe-doped Ni_2P and (e) 10% Fe-doped Ni_2P.

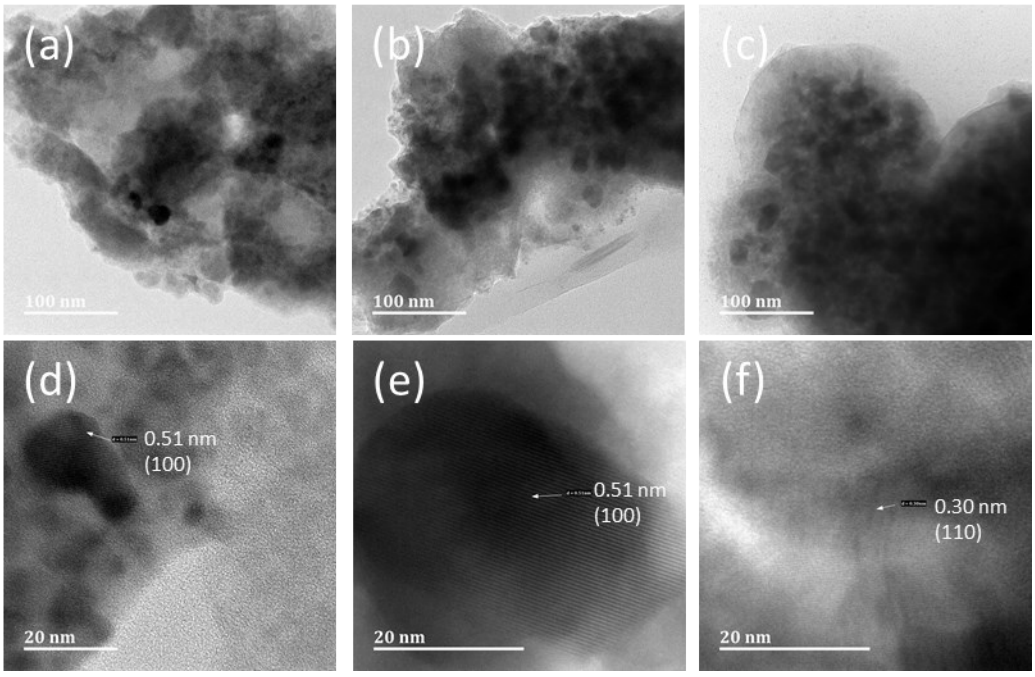

Figure S4: TEM images of (a) Ni_2P (b) 10% Co-Ni_2P and (c) 10% Fe-Ni_2P. HRTEM images of (d) Ni_2P (e) 10% Co-Ni_2P and (f) 10% Fe-Ni_2P.

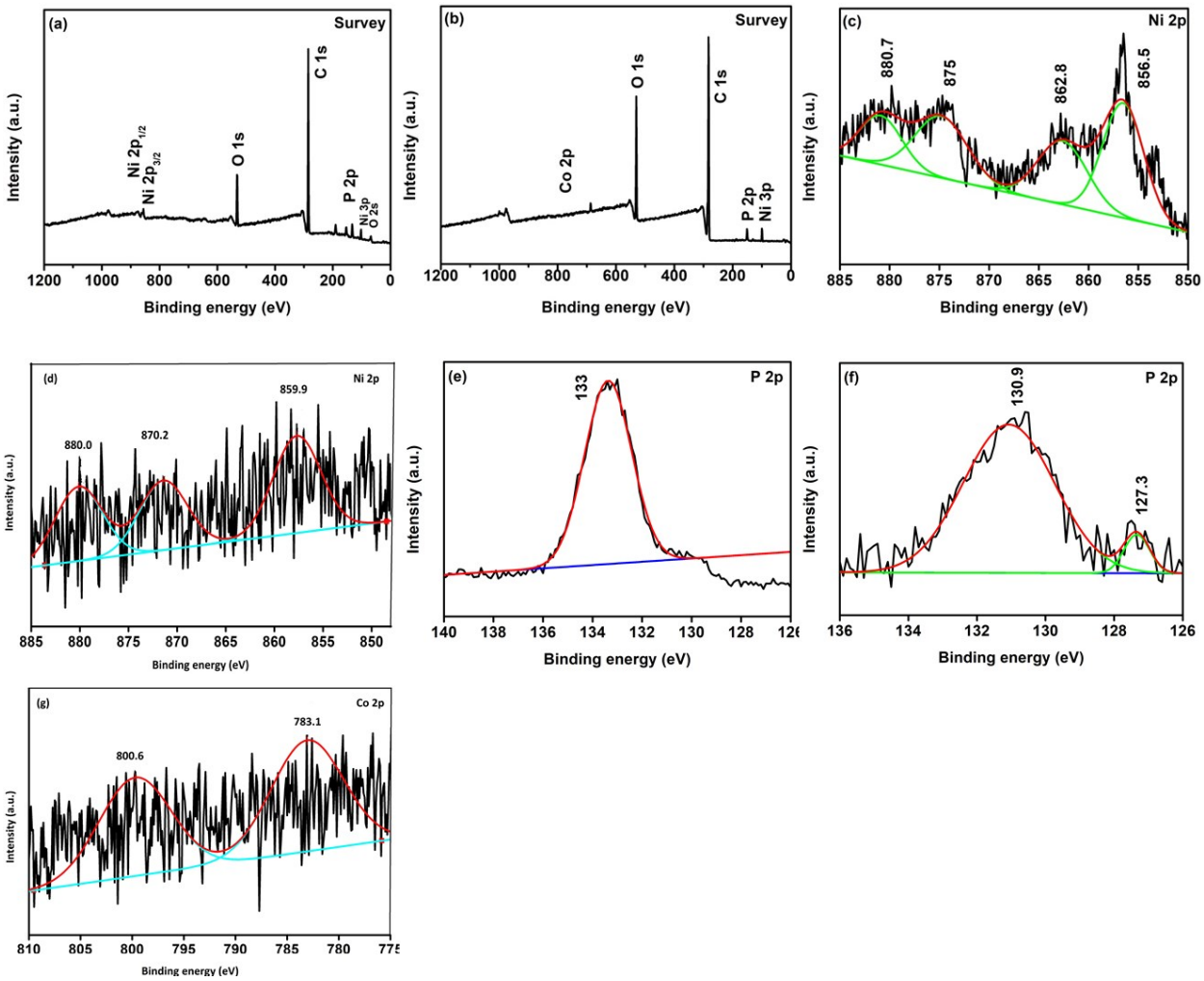

Figure S5: XPS survey spectra of (a) Ni_2P and (b) Co-Ni_2P. High resolution spectra of (c) Ni 2p of Ni_2P, (d) Ni 2p of Co-Ni_2P, (e) P 2p of Ni_2P, (f) P 2p of Co-Ni_2P and (f) Co 2p of Co-Ni_2P.

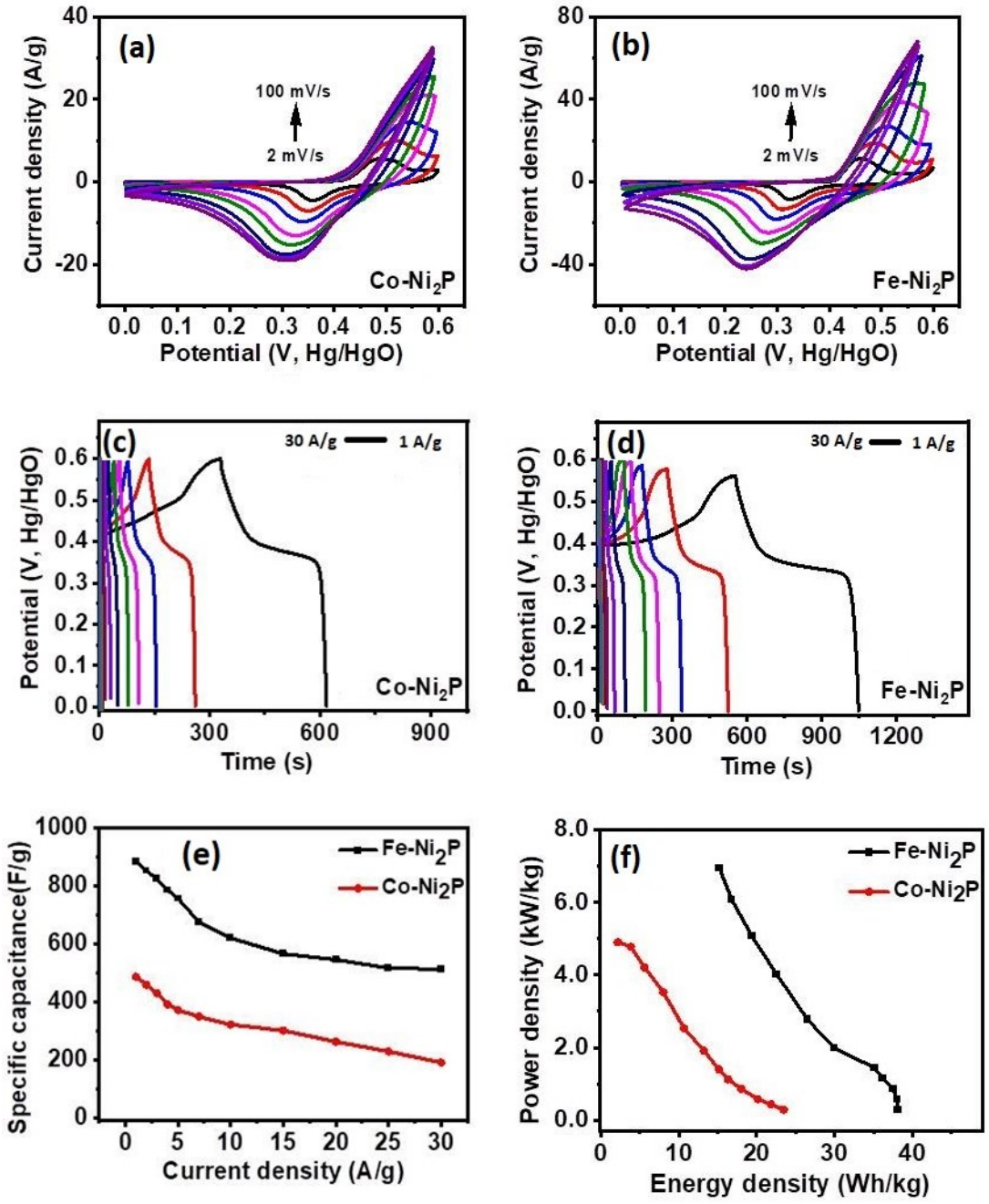

Figure S6: CV curves of (a) 5% Co-Ni_2P and (b) 5% Fe-Ni_2P electrodes, GCD curves of (c) 5% Co-Ni_2P and (b) 5% Fe-Ni_2P electrodes. Variation of (e) specific density as a function of current density and (f) power density as a function of energy density for 5% Co and Fe-Ni_2P electrodes.

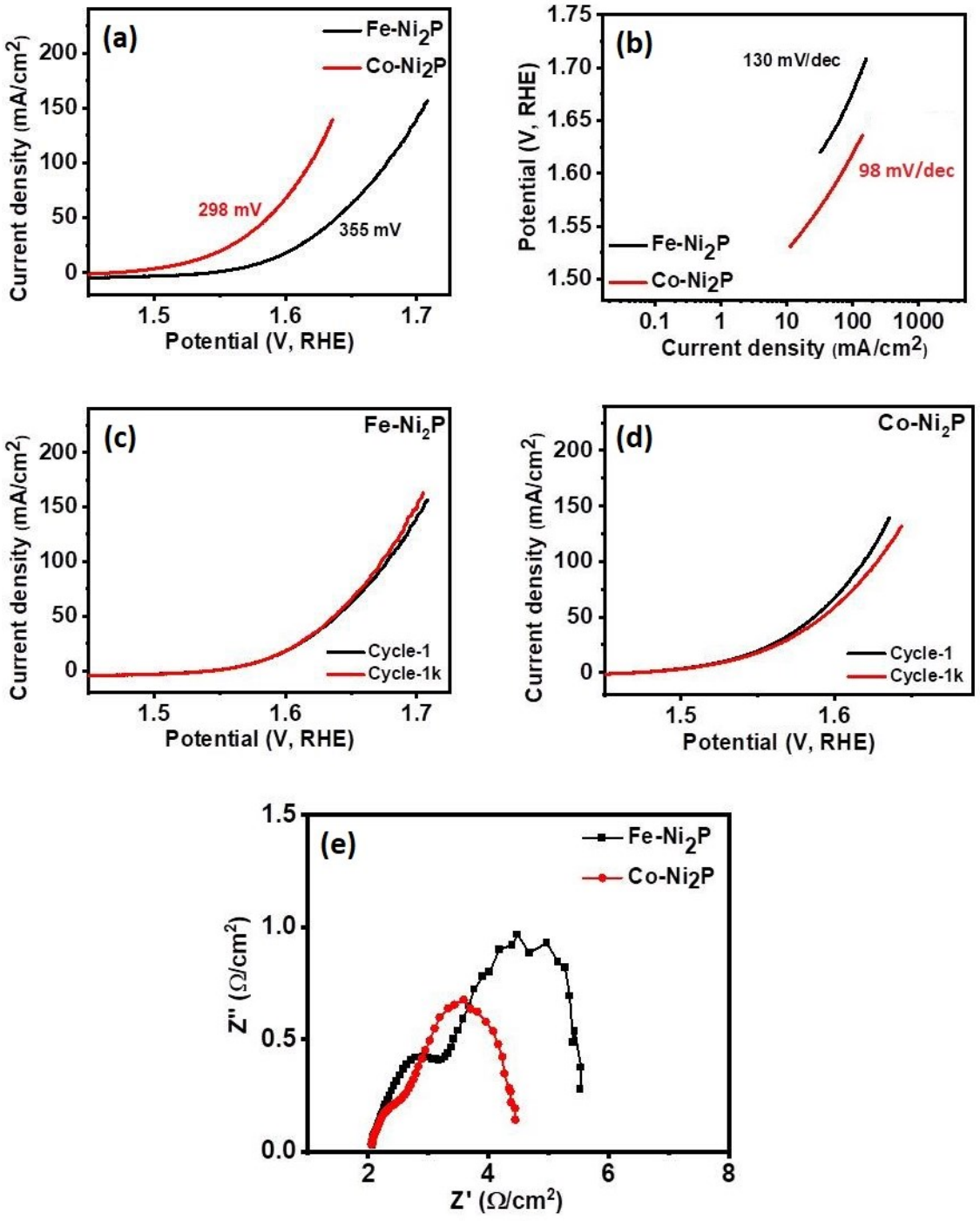

Figure S7: OER polarization curves (a) and Tafel slopes (b) for 5% Co and Fe-Ni_2P electrodes, OER polarization curves at different cycles for (c) 5% Fe-Ni_2P and (d) 5% Co-Ni_2P electrodes and Nyquist plot (e) for 5% Co and Fe-Ni_2P electrodes.

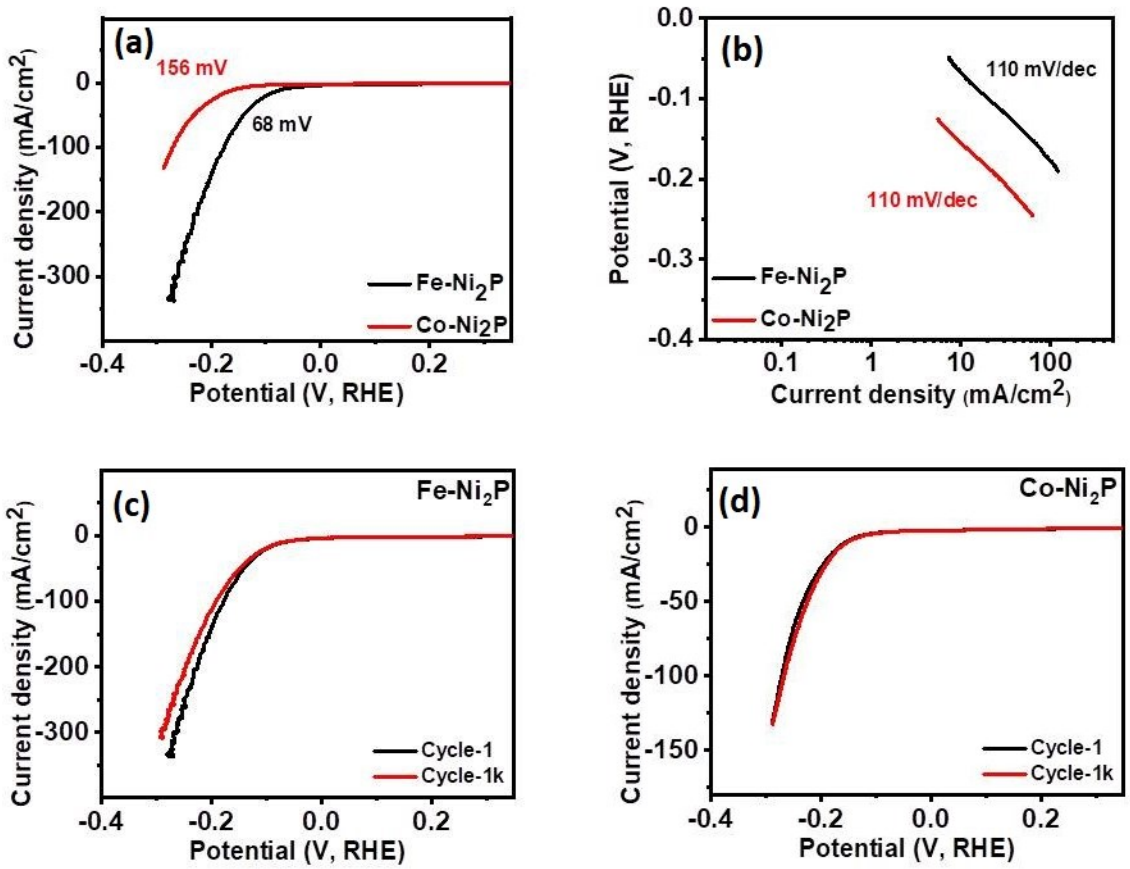

Figure S8: HER polarization curves (a) and Tafel slopes (b) for 5% Co and Fe-Ni_2P electrodes, HER polarization curves at different cycles for (c) 5% Fe-Ni_2P and (d) 5% Co-Ni_2P electrodes.

Table S1: A comparison of some nickel phosphide-based electrodes and our electrodes for supercapacitor applications.

Name	Voltage range	Specific capacitance (F/g)	Reference
Ni_2P (organic-phase strategy)	0-0.7V (V vs Hg/HgO)	418 F/g @ 1 A/g	[1]
Ni- coated Ni_2P	0-0.7V (V vs Hg/HgO)	581 F/g @ 1 A/g	[1]
Ni_5P_4	0-0.4V (V vs SCE)	801.5 F/g @ 1 A/g	[2]
PPy/Ni_2P	-0.4-0.4V (V vs SCE)	476.5 F/g @ 1 A/g	[3]
$Ni_2P_2O_7$ nanowire	0-0.4V (V vs Ag/AgCl)	772.5 F/g @ 1 A/g	[4]
Ni_2P nanoparticle	0-0.4V (V vs SCE)	600.1 F/g @ 1 A/g	[5]
5% graphene/Ni_2P nanoparticle	0-0.4V (V vs SCE)	672.4 F/g @ 1 A/g	[5]
Ni_2P	0-0.6V (V vs Hg/HgO)	674 F/g @ 1 A/g	This study
Co-Ni_2P	0-0.6V (V vs Hg/HgO)	864 F/g @ 1 A/g	This study
Fe-Ni_2P	0-0.6V (V vs Hg/HgO)	856 F/g @ 1 A/g	This study

Table S2: A comparison of some nickel phosphide-based electrodes and our electrodes for OER

Name	Overpotential (mV) @10 mA/cm2	Tafel slope (mV/dec)	Reference
Ni_2P nano particles	~ 500	70	[6]
Ni_2P nano wire	~ 400	60	[6]
Ni_2P-CoP	320	69	[7]
NiOOH/ Ni_5P_4	290	~40	[8]
NiCoP/C nanoboxes	330	96	[9]
NiCoP	280	87	[10]
Ni-P nanoplates	300	64	[11]
Ni_2P	340	103	This study
Co-Ni_2P	320	91	This study
Fe-Ni_2P	259	69	This study

Table S3: A comparison of some nickel phosphide-based electrodes and our electrodes for HER

Name	Overpotential	Tafel slope	Reference
Ni_2P@glassy carbon substrate	~ 270	84	[12]
$Ni_{12}P_5$@glassy carbon substrate	~ 450	108	[12]
MOF Ni_2P	~ 172	62	[13]
MOF $Ni_{12}P_5$	~ 670	270	[13]
Ni_2P/Carbon-nanosheets	174	64	[14]
Ni_2P particles	310	109	[15]
Ni_2P	164	117	This study
Co-Ni_2P	158	113	This study
Fe-Ni_2P	202	113	This study

References

(1) Lu, Y.; Liu, J.-k.; Liu, X.-y.; Huang, S.; Wang, T.-q.; Wang, X.-l.; Gu, C.-d.; Tu, J.-p.; Mao, S. X. Facile synthesis of Ni-coated Ni 2 P for supercapacitor applications. *CrystEngComm* **2013**, *15*, 7071-7079.

(2) Wang, D.; Kong, L. B.; Liu, M. C.; Luo, Y. C.; Kang, L. An Approach to Preparing Ni–P with Different Phases for Use as Supercapacitor Electrode Materials. *Chemistry–A European Journal* **2015**, *21*, 17897-17903.

(3) Liu, S.; Chen, Y.; Ren, J.; Wang, Y.; Wei, W. An effective interaction in polypyrrole/nickel phosphide (PPy/Ni 2 P) for high-performance supercapacitor. *Journal of Solid State Electrochemistry* **2019**, *23*, 3409-3418.

(4) Zhou, Y.; Liu, C.; Li, X.; Sun, L.; Wu, D.; Li, J.; Huo, P.; Wang, H. Chemical precipitation synthesis of porous Ni2P2O7 nanowires for supercapacitor. *Journal of Alloys and Compounds* **2019**, *790*, 36-41.

(5) Du, W.; Wei, S.; Zhou, K.; Guo, J.; Pang, H.; Qian, X. One-step synthesis and graphene-modification to achieve nickel phosphide nanoparticles with electrochemical properties suitable for supercapacitors. *Materials Research Bulletin* **2015**, *61*, 333-339.

(6) Han, A.; Chen, H.; Sun, Z.; Xu, J.; Du, P. High catalytic activity for water oxidation based on nanostructured nickel phosphide precursors. *Chemical Communications* **2015**, *51*, 11626-11629.

(7) Liang, X.; Zheng, B.; Chen, L.; Zhang, J.; Zhuang, Z.; Chen, B. MOF-derived formation of Ni2P–CoP bimetallic phosphides with strong interfacial effect toward electrocatalytic water splitting. *ACS Applied Materials & Interfaces* **2017**, *9*, 23222-23229.

(8) Ledendecker, M.; Krick Calderón, S.; Papp, C.; Steinrück, H. P.; Antonietti, M.; Shalom, M. The synthesis of nanostructured Ni5P4 films and their use as a non-noble bifunctional electrocatalyst for full water splitting. *Angewandte Chemie International Edition* **2015**, *54*, 12361-12365.

(9) He, P.; Yu, X. Y.; Lou, X. W. Carbon-incorporated nickel–cobalt mixed metal phosphide nanoboxes with enhanced electrocatalytic activity for oxygen evolution. *Angewandte Chemie International Edition* **2017**, *56*, 3897-3900.

(10) Liang, H.; Gandi, A. N.; Anjum, D. H.; Wang, X.; Schwingenschlögl, U.; Alshareef, H. N. Plasma-assisted synthesis of NiCoP for efficient overall water splitting. *Nano letters* **2016**, *16*, 7718-7725.

(11) Yu, X.-Y.; Feng, Y.; Guan, B.; Lou, X. W. D.; Paik, U. Carbon coated porous nickel phosphides nanoplates for highly efficient oxygen evolution reaction. *Energy & Environmental Science* **2016**, *9*, 1246-1250.

(12) Kucernak, A. R.; Sundaram, V. N. N. Nickel phosphide: the effect of phosphorus content on hydrogen evolution activity and corrosion resistance in acidic medium. *Journal of Materials Chemistry A* **2014**, *2*, 17435-17445.

(13) Tian, T.; Ai, L.; Jiang, J. Metal–organic framework-derived nickel phosphides as efficient electrocatalysts toward sustainable hydrogen generation from water splitting. *RSC Advances* **2015**, *5*, 10290-10295.

(14) Li, Y.; Cai, P.; Ci, S.; Wen, Z. Strongly Coupled 3D Nanohybrids with Ni2P/Carbon Nanosheets as pH-Universal Hydrogen Evolution Reaction Electrocatalysts. *ChemElectroChem* **2017**, *4*, 340-344.

(15) Yan, L.; Dai, P.; Wang, Y.; Gu, X.; Li, L.; Cao, L.; Zhao, X. In situ synthesis strategy for hierarchically porous Ni_2P polyhedrons from MOFs templates with enhanced electrochemical properties for hydrogen evolution. *ACS applied materials & interfaces* **2017**, *9*, 11642-11650.